Supporting Information

Phenoxido-Bridged Open-cubane [$Cu_4(\mu_3\text{-}OH)_2$] and Stepped-cubane [$Cu_4(\mu_3\text{-}OMe)_2$] Complexes from a Semicarbazone Schiff Base: Synthesis, Anion Coordination Tunable Structures, Biomimicking Functions, DNA Binding and Magnetic Behavior with Theoretical Supports

Anupama Manna[a], Mohammad Fawad Ansari[b], Farukh Arjmand[b], Zvonko Jagličić[c], Radovan Herchel[d], Debashis Ray[a*]

[a] *Department of Chemistry, Indian Institute of Technology Kharagpur, Kharagpur 721302, India*

[b] *Department of Chemistry, Aligarh Muslim University, Aligarh 202002, India*

[c] *Institute of Mathematics, Physics and Mechanics & Faculty of Civil and Geodetic Engineering, University of Ljubljana, Ljubljana 1000, Slovenia*

[d] *Department of Inorganic Chemistry, Faculty of Science, Palacký University, 17. listopadu 12, 77146 Olomouc, Czech Republic*

Email: dray@chem.iitkgp.ac.in

Contents

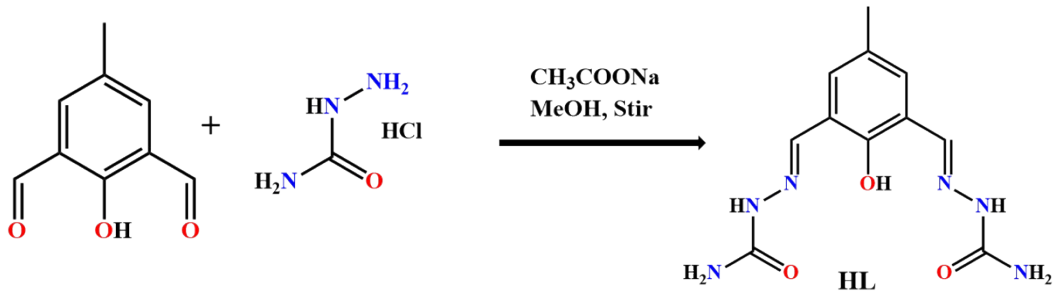

Scheme S1. Schematic representation for formation of HL

Table S1 Crystal data and structure refinement of **1** and **2**

Empirical formula	**1-** $C_{22}H_{38}Cl_4Cu_4N_{12}O_{29}$	**2-** $C_{24}H_{36}Cu_4N_{16}O_{22}$
Formula weight	1332.56	1154.89
Temperature/K	303.0	301.0
Crystal system	monoclinic	triclinic
Space group	$P2_1/n$	P-1
a/Å	13.9537(14)	8.185(4)
b/Å	25.080(2)	10.141(4)
c/Å	14.9365(14)	13.801(7)
α/°	90	85.22(3)
β/°	117.783(4)	79.67(3)
γ/°	90	66.51(3)
Volume/Å^3	4624.5(8)	1033.5(9)
Z	4	2
ρ_{calc}g/cm^3	1.914	1.855
μ/mm^{-1}	2.157	1.015
F(000)	2672.0	102.0
Radiation	Mo Kα (λ = 0.71073)	Mo Kα (λ = 0.71073)
2Θ range for data collection/°	5.46 to 50.02	5.528 to 50.244
Index ranges	-16 ≤ h ≤ 15, -29 ≤ k ≤ 29, -17 ≤ l ≤ 17	-9 ≤ h ≤ 9, -12 ≤ k ≤ 12, -16 ≤ l ≤ 16
Reflections collected	38566	12128
Independent reflections	8137 [R_{int} = 0.0401, R_{sigma} = 0.0303]	3590 [R_{int} = 0.1111, R_{sigma} = 0.1161]
Data/restraints/parameters	8137/0/657	3590/0/303
Goodness-of-fit on F^2	1.037	1.110
Final R indexes	R_1 = 0.0461, wR_2 = 0.1221	R_1 = 0.0641, wR_2 = 0.1059

[I>=2σ (I)]		
Final R indexes [all data]	R_1 = 0.0601, wR_2 = 0.1369	R_1 = 0.1295, wR_2 = 0.1186

Table S2. Selected interatomic distances (Å) of complex **1**

Atom	Atom	Length/Å		Atom	Atom	Length/Å
Cu2	Cu1	2.9157(8)		N10	C19	1.279(6)
Cu2	O10	1.925(3)		N4	N5	1.379(5)
Cu2	O9	2.303(3)		N4	C9	1.288(6)
Cu2	O2	1.958(3)		N11	C21	1.339(6)
Cu2	O1	1.943(3)		N7	N8	1.376(6)
Cu2	N1	1.923(4)		N7	C20	1.283(6)
Cu1	O10	1.911(3)		N2	C10	1.351(6)
Cu1	O1	1.941(3)		N5	C11	1.356(6)
Cu1	O3	1.965(3)		N12	C21	1.330(6)
Cu1	O7	2.392(4)		N6	C11	1.316(6)
Cu1	N4	1.925(4)		N8	C22	1.372(7)
Cu4	Cu3	2.9099(8)		C5	C6	1.413(6)
Cu4	O9	1.927(3)		C5	C4	1.405(6)
Cu4	O5	1.967(3)		N3	C10	1.311(6)
Cu4	O4	1.945(3)		C9	C6	1.450(7)
Cu4	N10	1.931(4)		C17	C16	1.404(7)
Cu4	O8	2.311(4)		C17	C19	1.473(7)
Cu3	O10	2.418(4)		C17	C18	1.391(7)
Cu3	O9	1.946(3)		C16	C15	1.408(6)
Cu3	O6	1.943(3)		C6	C7	1.412(7)
Cu3	O4	1.936(3)		C4	C8	1.446(7)
Cu3	N7	1.924(4)		C4	C3	1.396(6)
Cl2	O17	1.410(4)		C3	C2	1.373(8)
Cl2	O16	1.432(4)		C20	C15	1.445(7)
Cl2	O15	1.425(5)		N9	C22	1.315(7)
Cl2	O18	1.432(5)		C15	C14	1.408(7)
Cl1	O11	1.411(5)		C18	C13	1.393(7)
Cl1	O12	1.405(6)		C13	C14	1.376(8)
Cl1	O13	1.376(6)		C13	C12	1.520(7)
Cl1	O14	1.412(7)		C2	C7	1.369(8)
O5	C21	1.271(6)		C2	C1	1.524(7)
O2	C10	1.269(5)		Cl4	O24	1.337(9)
O1	C5	1.340(5)		Cl4	O26	1.284(10)
O3	C11	1.261(5)		Cl4	O25	1.292(9)
O6	C22	1.242(6)		Cl4	O23	1.271(15)

O4	C16	1.340(5)		Cl3	O19	1.441(9)
N1	N2	1.371(5)		Cl3	O22	1.282(7)
N1	C8	1.291(6)		Cl3	O20	1.353(7)
N10	N11	1.383(5)		Cl3	O21	1.351(9)

Table S3. Selected bond angles (°) of complex **1**

Atom	**Atom**	**Atom**	**Angle/°**		**Atom**	**Atom**	**Atom**	**Angle/°**
O10	Cu2	Cu1	40.35(10)		Cu1	O1	Cu2	97.29(13)
O9	Cu2	Cu1	93.82(9)		C5	O1	Cu2	130.5(3)
O9	Cu2	O10	86.11(14)		C5	O1	Cu1	130.2(3)
O2	Cu2	Cu1	142.94(9)		C11	O3	Cu1	111.7(3)
O2	Cu2	O10	105.04(13)		C22	O6	Cu3	112.3(3)
O2	Cu2	O9	96.53(13)		Cu3	O4	Cu4	97.17(15)
O1	Cu2	Cu1	41.34(9)		C16	O4	Cu4	127.9(3)
O1	Cu2	O10	81.13(13)		C16	O4	Cu3	130.4(3)
O1	Cu2	O9	91.79(13)		N2	N1	Cu2	110.6(3)
O1	Cu2	O2	169.92(14)		C8	N1	Cu2	129.5(3)
N1	Cu2	Cu1	130.40(11)		C8	N1	N2	120.0(4)
N1	Cu2	O10	170.13(16)		N11	N10	Cu4	110.7(3)
N1	Cu2	O9	99.18(14)		C19	N10	Cu4	128.5(3)
N1	Cu2	O2	82.75(14)		C19	N10	N11	120.6(4)
N1	Cu2	O1	90.34(14)		N5	N4	Cu1	110.5(3)
O10	Cu1	Cu2	40.72(10)		C9	N4	Cu1	129.5(3)
O1	Cu1	Cu2	41.37(9)		C9	N4	N5	120.0(4)
O1	Cu1	O10	81.53(13)		C21	N11	N10	114.9(4)
O3	Cu1	Cu2	144.80(9)		N8	N7	Cu3	110.9(3)
O3	Cu1	O10	104.14(14)		C20	N7	Cu3	128.8(3)
O3	Cu1	O1	168.23(14)		C20	N7	N8	120.3(4)
O7	Cu1	Cu2	94.18(10)		C10	N2	N1	115.7(4)
O7	Cu1	O10	96.79(15)		C11	N5	N4	115.4(4)
O7	Cu1	O1	97.54(14)		C22	N8	N7	113.8(4)
O7	Cu1	O3	92.07(15)		C6	C5	O1	120.2(4)
N4	Cu1	Cu2	131.19(12)		C4	C5	O1	120.9(4)
N4	Cu1	O10	167.37(16)		C4	C5	C6	118.9(4)
N4	Cu1	O1	89.83(14)		N5	C11	O3	119.5(4)
N4	Cu1	O3	82.80(14)		N6	C11	O3	122.5(5)
N4	Cu1	O7	93.45(16)		N6	C11	N5	118.0(4)
O9	Cu4	Cu3	41.55(10)		C6	C9	N4	123.9(4)
O5	Cu4	Cu3	144.74(10)		C19	C17	C16	124.5(4)
O5	Cu4	O9	103.34(14)		C18	C17	C16	119.5(4)
O4	Cu4	Cu3	41.30(9)		C18	C17	C19	116.0(4)
O4	Cu4	O9	81.50(13)		C17	C16	O4	120.3(4)
O4	Cu4	O5	170.34(15)		C15	C16	O4	120.4(4)

N10	Cu4	Cu3	131.69(11)		C15	C16	C17	119.3(4)
N10	Cu4	O9	163.19(16)		C17	C19	N10	123.6(4)
N10	Cu4	O5	82.68(14)		N11	C21	O5	120.7(4)
N10	Cu4	O4	90.44(14)		N12	C21	O5	121.0(4)
O8	Cu4	Cu3	88.78(11)		N12	C21	N11	118.3(4)
O8	Cu4	O9	102.37(15)		C9	C6	C5	124.3(4)
O8	Cu4	O5	98.90(15)		C7	C6	C5	118.6(4)
O8	Cu4	O4	88.05(16)		C7	C6	C9	117.1(4)
O8	Cu4	N10	92.00(16)		C8	C4	C5	124.5(4)
O10	Cu3	Cu4	91.12(9)		C3	C4	C5	119.1(4)
O9	Cu3	Cu4	41.05(9)		C3	C4	C8	116.3(4)
O9	Cu3	O10	82.53(13)		N2	C10	O2	119.1(4)
O6	Cu3	Cu4	144.15(11)		N3	C10	O2	122.4(4)
O6	Cu3	O10	95.09(14)		N3	C10	N2	118.5(4)
O6	Cu3	O9	104.91(14)		C4	C8	N1	124.1(4)
O4	Cu3	Cu4	41.53(9)		C2	C3	C4	123.1(5)
O4	Cu3	O10	86.86(14)		C15	C20	N7	124.5(4)
O4	Cu3	O9	81.24(13)		C20	C15	C16	124.8(4)
O4	Cu3	O6	173.73(14)		C14	C15	C16	119.0(5)
N7	Cu3	Cu4	129.78(12)		C14	C15	C20	116.2(4)
N7	Cu3	O10	103.50(15)		C13	C18	C17	121.9(5)
N7	Cu3	O9	169.91(15)		N8	C22	O6	120.0(4)
N7	Cu3	O6	82.83(16)		N9	C22	O6	121.8(5)
N7	Cu3	O4	90.92(15)		N9	C22	N8	118.2(5)
O16	Cl2	O17	109.9(3)		C14	C13	C18	118.1(5)
O15	Cl2	O17	110.7(3)		C12	C13	C18	120.7(5)
O15	Cl2	O16	108.5(3)		C12	C13	C14	121.1(5)
O18	Cl2	O17	110.1(3)		C7	C2	C3	117.6(4)
O18	Cl2	O16	109.5(3)		C1	C2	C3	121.3(5)
O18	Cl2	O15	108.1(3)		C1	C2	C7	121.1(5)
O12	Cl1	O11	109.7(4)		C2	C7	C6	122.7(5)
O13	Cl1	O11	110.6(4)		C13	C14	C15	122.0(5)
O13	Cl1	O12	112.2(5)		O26	Cl4	O24	108.4(8)
O14	Cl1	O11	110.9(5)		O25	Cl4	O24	113.4(7)
O14	Cl1	O12	108.9(5)		O25	Cl4	O26	115.5(9)
O14	Cl1	O13	104.4(6)		O23	Cl4	O24	104.5(12)
Cu1	O10	Cu2	98.93(16)		O23	Cl4	O26	110.8(14)
Cu3	O10	Cu2	93.21(14)		O23	Cl4	O25	103.7(11)
Cu3	O10	Cu1	109.11(15)		O22	Cl3	O19	105.8(7)
Cu4	O9	Cu2	108.63(15)		O20	Cl3	O19	106.0(6)
Cu3	O9	Cu2	96.28(14)		O20	Cl3	O22	113.1(6)
Cu3	O9	Cu4	97.41(15)		O21	Cl3	O19	99.4(8)
C21	O5	Cu4	111.0(3)		O21	Cl3	O22	119.5(9)
C10	O2	Cu2	111.7(3)		O21	Cl3	O20	111.1(8)

Table S4. Selected interatomic distances (Å) of complex **2**

Atom	Atom	Length/Å		Atom	Atom	Length/Å
Cu1	Cu2	2.8836(16)		N4	N5	1.371(6)
Cu1	O1	1.936(4)		N4	C8	1.284(7)
Cu1	O2	1.960(4)		N2	C11	1.363(7)
Cu1	O4	1.942(4)		N6	C9	1.315(7)
Cu1	O7	2.380(4)		N8	O10	1.245(7)
Cu1	N1	1.926(5)		N8	O8	1.208(7)
Cu2	O1	1.936(4)		N8	O9	1.235(7)
Cu2	O3	1.954(4)		N3	C11	1.313(7)
Cu2	O4	1.930(4)		N5	C9	1.359(7)
Cu2	O5	2.405(5)		O6	N7	1.252(7)
Cu2	N4	1.931(5)		C8	C6	1.448(8)
O1	C5	1.337(6)		C5	C4	1.410(7)
O2	C11	1.271(7)		C5	C6	1.409(8)
O3	C9	1.264(7)		C4	C10	1.457(8)
O4	Cu11	2.380(4)		C4	C3	1.405(7)
O4	C12	1.464(8)		C7	C2	1.385(8)
N1	N2	1.377(6)		C7	C6	1.398(8)
N1	C10	1.290(7)		C2	C3	1.370(8)
O5	N7	1.250(6)		C2	C1	1.513(8)
O7	N7	1.252(7)				

Table S5. Selected angles (°) of complex **2**

Atom	Atom	Atom	Angle/°		Atom	Atom	Atom	Angle/°
O1	Cu1	Cu2	41.86(11)		C12	O4	Cu11	115.3(4)
O1	Cu1	O2	174.11(16)		C12	O4	Cu2	120.6(4)
O1	Cu1	O4	82.54(16)		N2	N1	Cu1	111.3(3)
O1	Cu1	O7	94.26(15)		C10	N1	Cu1	128.3(4)
O2	Cu1	Cu2	143.65(12)		C10	N1	N2	120.3(5)
O2	Cu1	O41	87.43(16)		N7	O5	Cu2	117.2(4)
O41	Cu1	Cu2	95.17(9)		N5	N4	Cu2	110.7(4)
O4	Cu1	Cu2	41.71(11)		C8	N4	Cu2	128.6(4)
O4	Cu1	O2	103.28(16)		C8	N4	N5	120.6(5)
O4	Cu1	O7	82.79(16)		C11	N2	N1	114.8(5)
N1	Cu1	Cu2	131.67(14)		O8	N8	O10	121.2(6)
N1	Cu1	O1	91.49(18)		O8	N8	O9	120.1(7)
N1	Cu1	O2	82.64(18)		O9	N8	O10	118.7(6)
N1	Cu1	O4	172.97(18)		C9	N5	N4	114.9(5)
N1	Cu1	O7	101.45(18)		O5	N7	O7	120.3(6)
O1	Cu2	Cu1	41.86(11)		O5	N7	O6	119.5(6)
O1	Cu2	O3	171.58(18)		O7	N7	O6	120.2(6)

O1	Cu2	O5	88.14(17)		O2	C11	N2	119.3(5)
O3	Cu2	Cu1	145.06(13)		O2	C11	N3	121.4(6)
O3	Cu2	O5	96.97(17)		N3	C11	N2	119.3(6)
O4	Cu2	Cu1	42.01(11)		N4	C8	C6	124.5(6)
O4	Cu2	O1	82.84(16)		O3	C9	N6	122.5(6)
O4	Cu2	O3	103.29(16)		O3	C9	N5	119.9(5)
O4	Cu2	O5	94.87(17)		N6	C9	N5	117.5(6)
O4	Cu2	N4	171.61(19)		O1	C5	C4	120.7(5)
O5	Cu2	Cu1	84.77(11)		O1	C5	C6	121.0(5)
N4	Cu2	Cu1	132.04(15)		C6	C5	C4	118.3(5)
N4	Cu2	O1	90.45(18)		C5	C4	C10	124.8(5)
N4	Cu2	O3	82.90(19)		C3	C4	C5	118.9(5)
N4	Cu2	O5	89.9(2)		C3	C4	C10	116.2(5)
Cu2	O1	Cu1	96.28(17)		C2	C7	C6	122.4(6)
C5	O1	Cu1	129.6(3)		N1	C10	C4	124.1(5)
C5	O1	Cu2	129.0(4)		C7	C2	C1	121.6(6)
C11	O2	Cu1	112.0(4)		C3	C2	C7	117.1(6)

Table S6. Results of continuous shape measurement calculation using program SHAPE 2.1 for Cu1- Cu4 of complex **1** and Cu1-Cu2 of complex **2**

Metal ion	SPY-5	TBPY-5	vOC-5	PP-5	
Cu1 of 1	**1.054**	6.207	1.906	29.722	
Cu 2 of 1	**1.382**	6.374	1.599	28.030	
Cu 3 of 1	**1.916**	6.353	2.125	27.679	
Cu 4 of 1	**1.117**	5.109	1.822	29.890	
Cu1 of 2	**1.181**	6.485	1.532	31.357	
	JPPY-6	TPR-6	OC-6	PPY-6	HP-6
Cu2 of 2	26.554	15.175	**2.314**	24.489	27.258

SPY-5	4 C4v	Spherical square pyramid
TBPY-5	3 D3h	Trigonal bipyramid
vOC-5	2 C4v	Vacant octahedron
PP-5	1 D5h	Pentagon
JPPY-6	5 C5v	Johnson pentagonal pyramid J2
TPR-6	4 D3h	Trigonal prism
OC-6	3 Oh	Octahedron
PPY-6	2 C5v	Pentagonal pyramid
HP-6	1 D6h	Hexagon

Table S7. BVS analysis of the metal ion centers of **1**

Bond valence = exp [($R_0 - d_{ij}$) / b], R_0 = 1.504 for Cu^I – O, 1.61 for Cu^I – N, 1.655 for Cu^{II} – O and 1.713 for Cu^{II} – N, b = 0.37

Bond	**Bond length /A**	**BVS calculated by Cu^I – O/N R_0 parameters**	**BVS calculated by Cu^{II} – O/N R_0 parameters**
Cu1–O10	1.911(3)	0.332	0.500
Cu1–O1	1.941(3)	0.306	0.461
Cu1–O3	1.965(3)	0.287	0.432
Cu1–O7	2.392(4)	0.090	0.136
Cu1–N4	1.925(4)	0.426	0.563
		$\Sigma v(Cu^I) = 1.441$	**$\Sigma v(Cu^{II}) = 2.092$**

Bond	**Bond length /A**	**BVS calculated by Cu^I – O/N R_0 parameters**	**BVS calculated by Cu^{II} – O/N R_0 parameters**
Cu2–O10	1.925(3)	0.32	0.482
Cu2–O9	2.303(3)	0.115	0.173
Cu2–O2	1.958(3)	0.293	0.440
Cu2–O1	1.943(3)	0.305	0.459
Cu2–N1	1.923(4)	0.429	0.566
		$\Sigma v(Cu^I) = 1.462$	**$\Sigma v(Cu^{II}) = 2.12$**

Bond	**Bond length /A**	**BVS calculated by Cu^I – O/N R_0 parameters**	**BVS calculated by Cu^{II} – O/N R_0 parameters**
Cu3–O10	2.418(4)	0.084	0.127
Cu3–O9	1.946(3)	0.302	0.455
Cu3–O6	1.943(3)	0.305	0.459
Cu3–O4	1.936(3)	0.311	0.467
Cu3–N7	1.924(4)	0.427	0.565
		$\Sigma v(Cu^I) = 1.429$	**$\Sigma v(Cu^{II}) = 2.073$**

Bond	Bond length /A	BVS calculated by Cu^{I} – O/N R_0 parameters	BVS calculated by Cu^{II} – O/N R_0 parameters
Cu4–O9	1.927(3)	0.318	0.479
Cu4–O5	1.967(3)	0.286	0.430
Cu4–O4	1.945(3)	0.303	0.456
Cu4–O8	2.311(4)	0.112	0.169
Cu4–N10	1.931(4)	0.419	0.582
		$\Sigma v(Cu^{I}) = 1.438$	**$\Sigma v(Cu^{II}) = 2.116$**

Table S8. BVS analysis of the metal ion centers of **2**

Bond	Bond length /A	BVS calculated by Cu^{I} – O/N R_0 parameters	BVS calculated by Cu^{II} – O/N R_0 parameters
Cu1–O1	1.936(4)	O.311	0.467
Cu1–O2	1.960(4)	0.291	0.438
Cu1–O4	1.942(4)	0.306	0.460
Cu1–O7	2.380(4)	0.093	0.140
Cu1–N1	1.926(5)	0.425	0.562
		$\Sigma v(Cu^{I}) = 1.426$	**$\Sigma v(Cu^{II}) = 2.067$**

Bond	Bond length /A	BVS calculated by Cu^{I} – O/N R_0 parameters	BVS calculated by Cu^{II} –O /N R_0 parameters
Cu2–O1	1.936(4)	0.311	0.467
Cu2–O3	1.954(4)	0.296	0.445
Cu2–O4	1.930(4)	0.316	0.475
Cu2–O5	2.405(5)	0.087	0.131
Cu2–N4	1.931(5)	0.419	0.582
		$\Sigma v(Cu^{I}) = 1.429$	**$\Sigma v(Cu^{II}) = 2.1$**

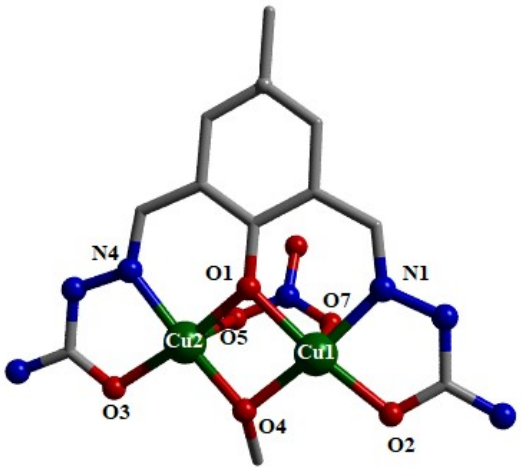

Figure S1. Asymmetric unit of Complex **2**

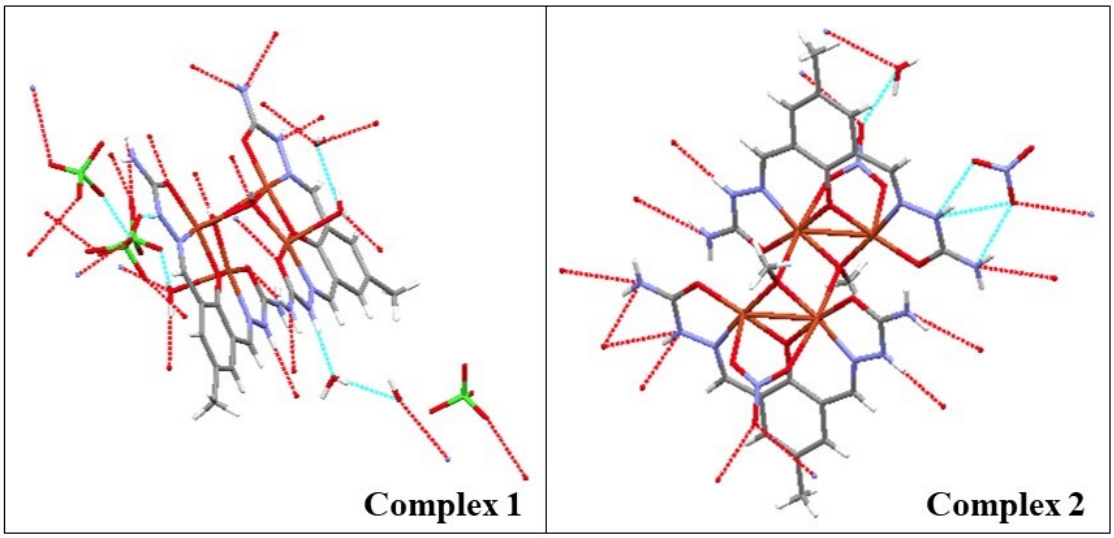

Figure S2. H- bonding interaction of complex **1** and **2**

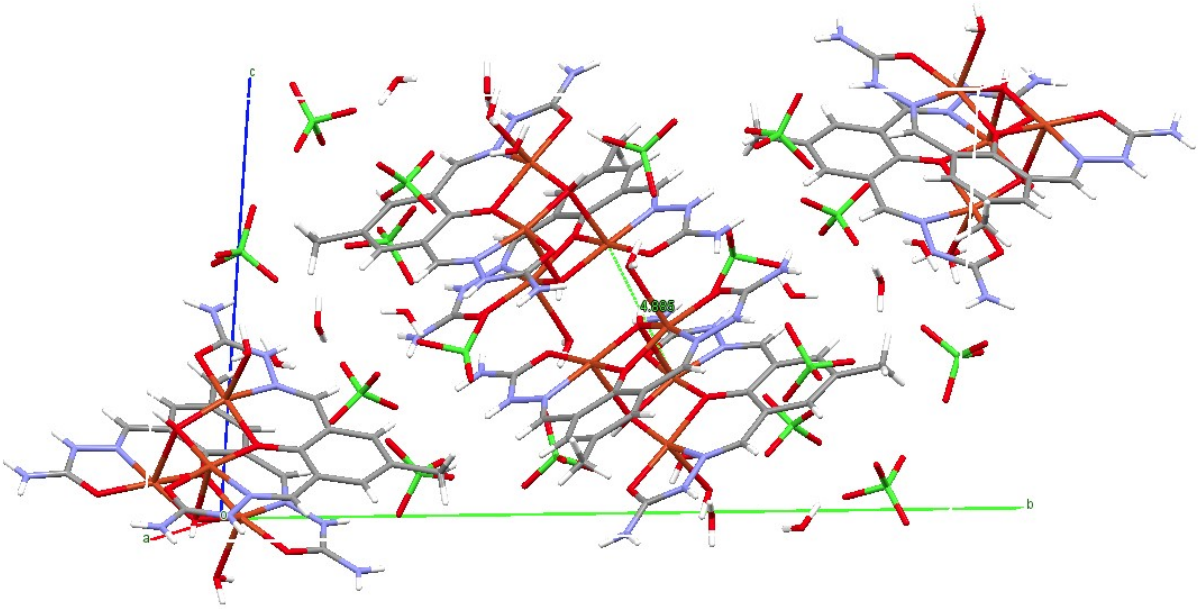

Figure S3. Molecular packing diagram of **Complex 1**

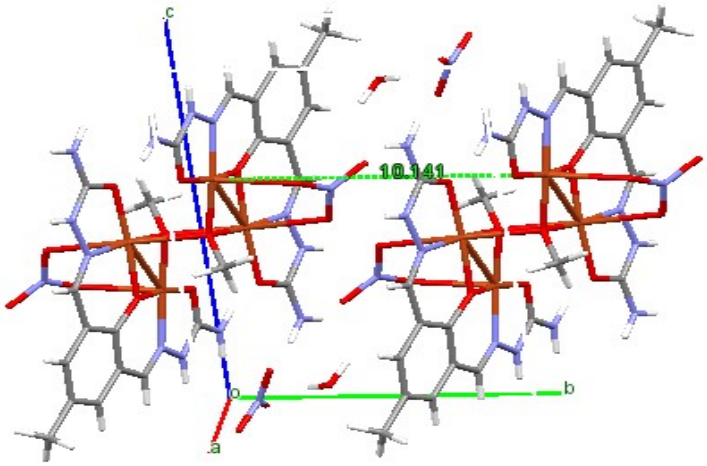

Figure S4. Molecular packing diagram of **Complex 2**

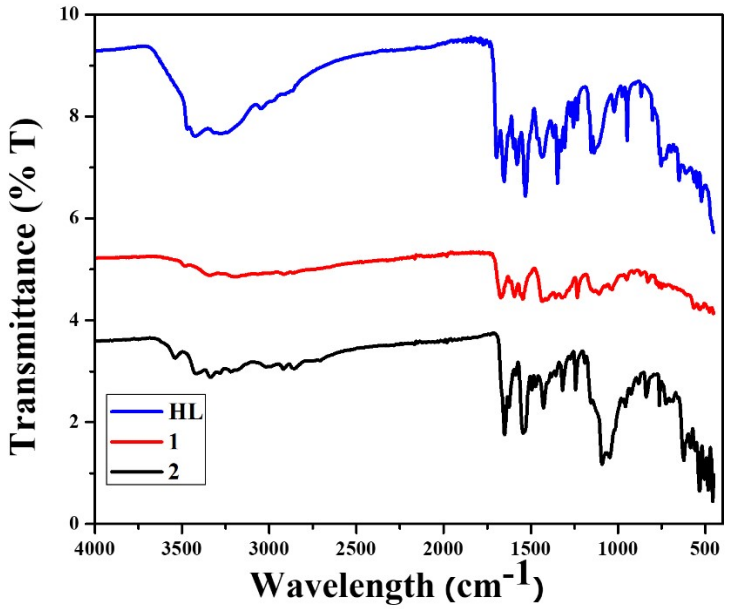

Figure S5. FTIR Spectra of **HL and 1** and **2**

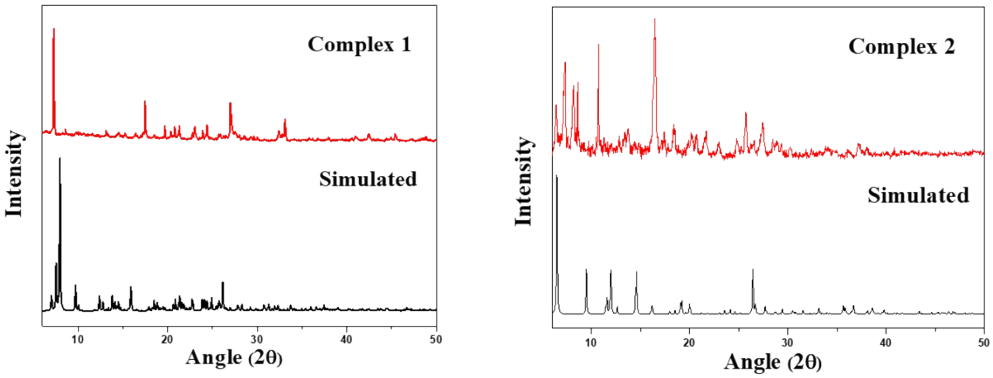

Figure S6. Powder XRD patterns of Complexes **1** and **2**

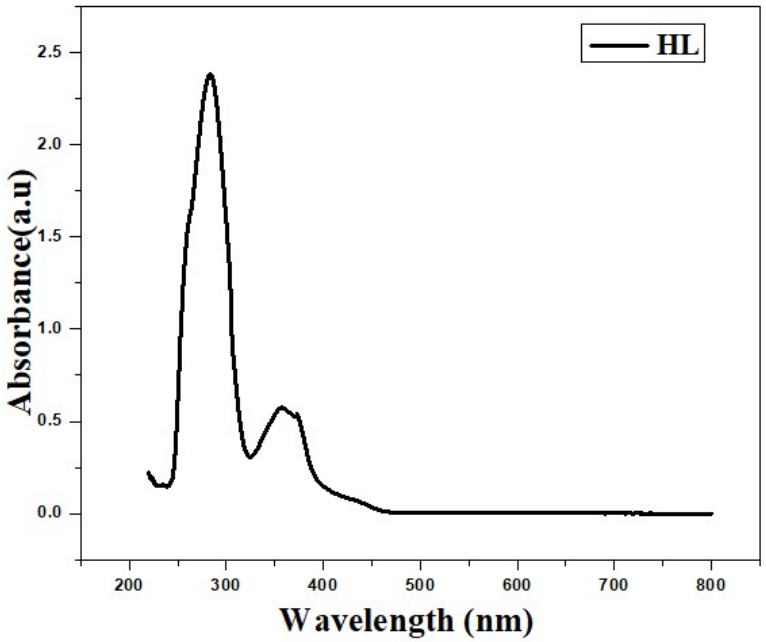

Figure S7. UV-Vis spectra of **HL** in DMF

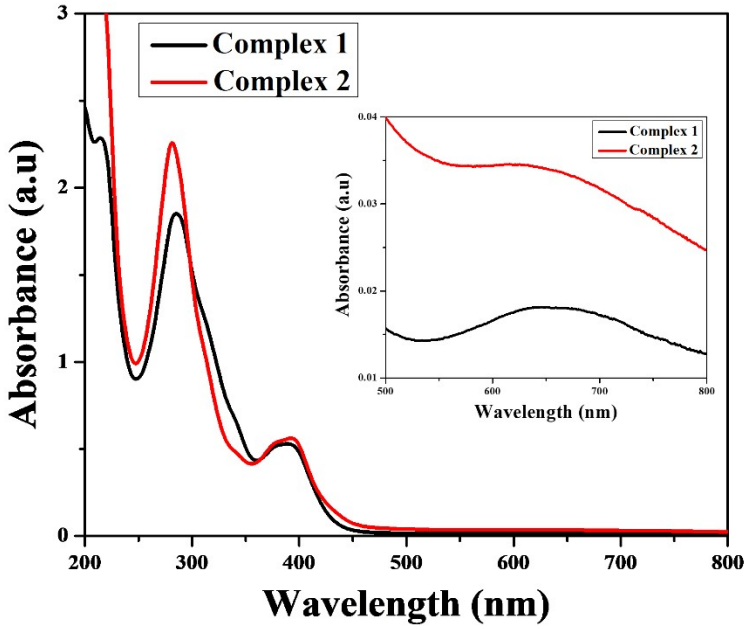

Figure S8. UV-Vis spectra of complexes **1** and **2** in MeOH: MeCN (1:1)

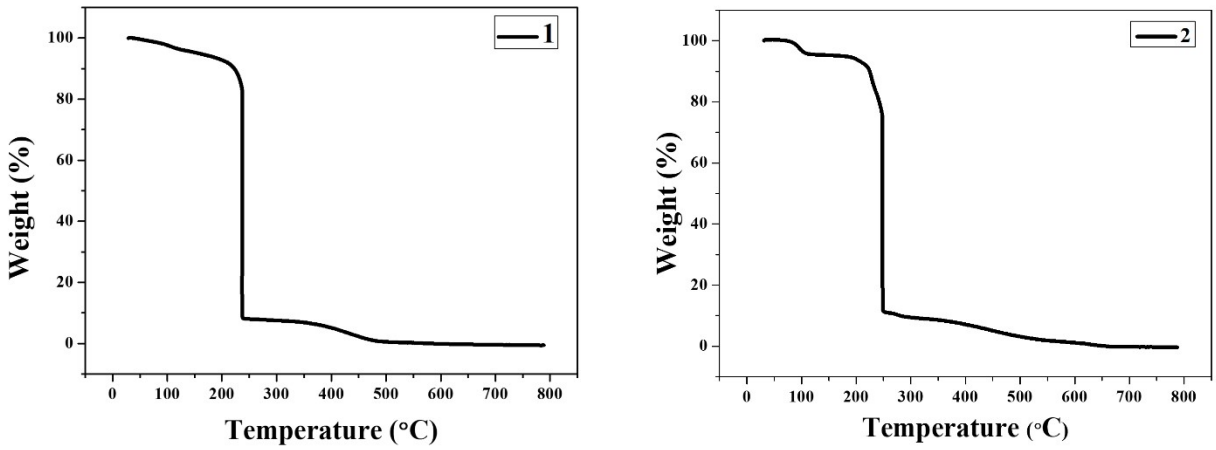

Figure S9. TGA plots of complex **1** and **2**

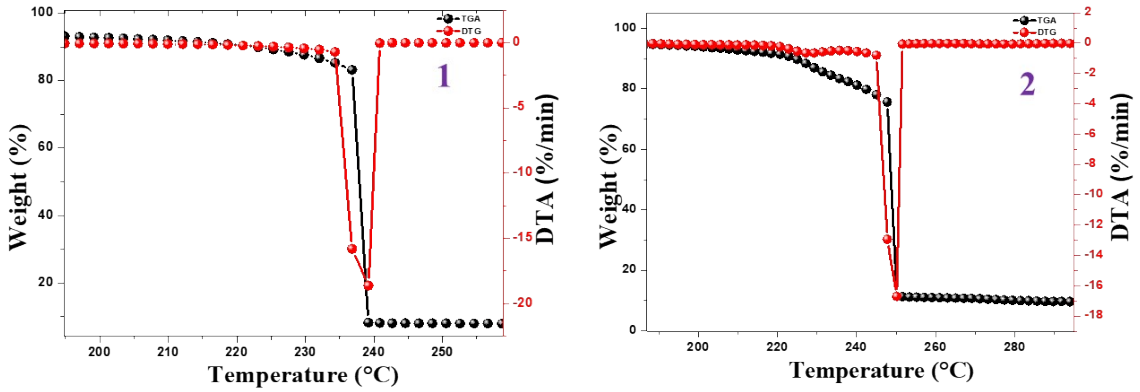

Figure S10. Combined TGA-DTA plots of complex **1** and **2**

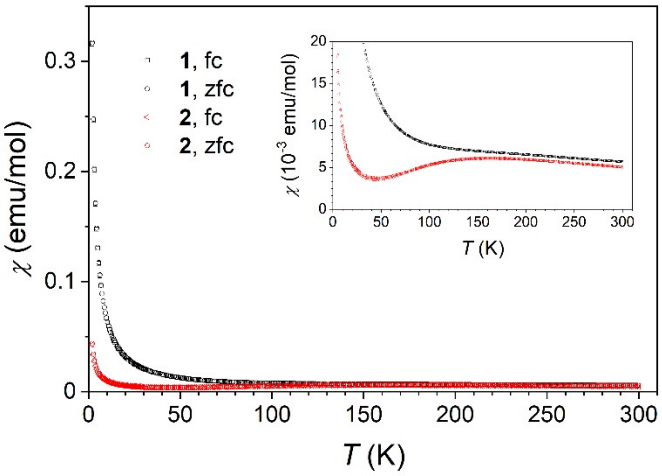

Figure S11. Temperature-dependent susceptibility of **1** and **2** measured in magnetic field of 1 kOe

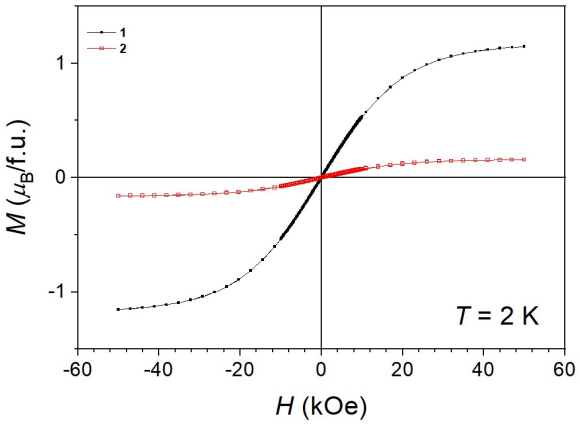

Figure S12. Magnetization curves of **1** and **2** at 2 K.

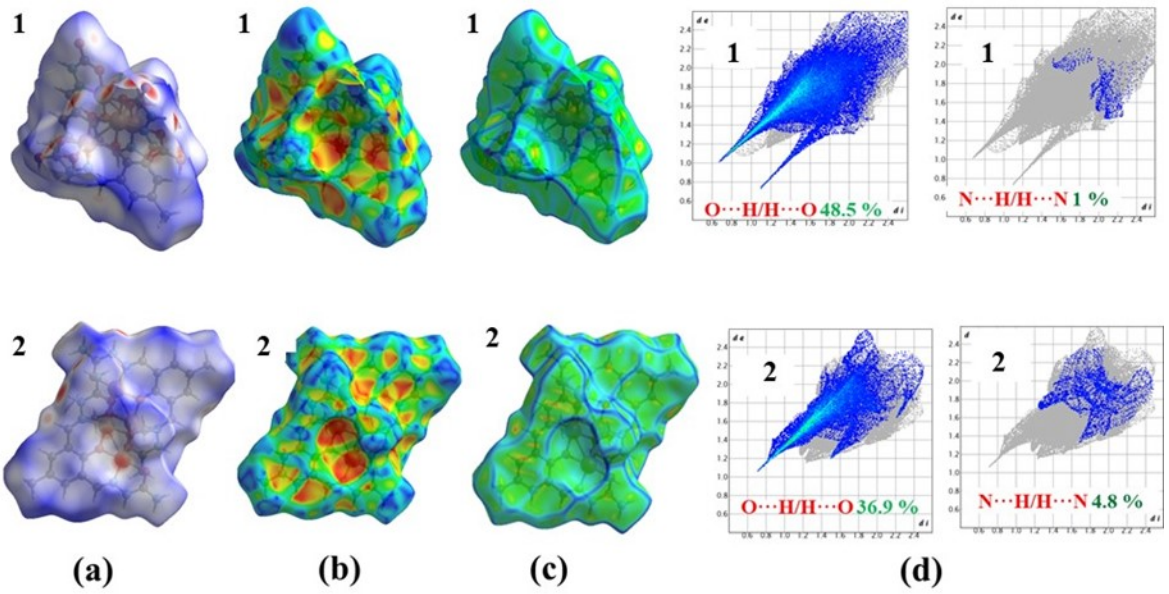

Figure S13. (a) Hirshfeld surfaces of the complexes; (b) shape index for the same complexes; (c) curvedness for the same complexes; (d) Fingerprint plot of the complexes resolved into (O···H/H···O) and (N···H/H···N) interactions of the complexes **1** and **2**

Table S9. The energy differences between BS-DFT spin states and the high-spin state in cm^{-1} for complex **1** (a), the difference between ($\varepsilon_{BS,i}$ - ε_{HS}) calculated with the help of derived J-parameters and actual BS-DFT values (b), and their relative errors (c)

a) $(\varepsilon_{BS,i} - \varepsilon_{HS})^{BS\text{-}DFT}$:

BS-state	PBE0	CAM-B3LYP	ωr²SCAN	B3LYP
1	-156.042	-141.190	-185.891	-227.071
2	-159.794	-138.480	-183.828	-219.426
3	-79.848	-64.506	-89.883	-117.733
4	-79.289	-64.934	-88.877	-118.545
12	3.113	4.002	4.811	6.624
13	-240.468	-206.666	-280.220	-357.187
14	-239.203	-197.401	-272.635	-341.250
23	-235.473	-202.064	-273.133	-333.215

b) $(\varepsilon_{BS,i} - \varepsilon_{HS})^{J} - (\varepsilon_{BS,i} - \varepsilon_{HS})^{BS\text{-}DFT}$:

BS-state	PBE0	CAM-B3LYP	ωr²SCAN	B3LYP
1	0.043	1.033	0.029	-0.772
2	0.043	1.033	0.029	-0.772

3	0.043	1.033	0.029	-0.772
4	0.043	1.033	0.029	-0.772
12	-0.043	-1.033	-0.029	0.772
13	-0.043	-1.033	-0.029	0.772
14	1.843	-2.848	-0.263	4.404
23	-1.886	1.815	0.235	-3.631

c) $[(\varepsilon_{BS,i} - \varepsilon_{HS})^{J} - (\varepsilon_{BS,i} - \varepsilon_{HS})^{BS\text{-}DFT}]/(\varepsilon_{BS,i} - \varepsilon_{HS})^{BS\text{-}DFT}$ (%):

BS-state	PBE0	CAM-B3LYP	ωr^{2}SCAN	B3LYP
1	0.0%	-0.7%	0.0%	0.3%
2	0.0%	-0.7%	0.0%	0.4%
3	-0.1%	-1.6%	0.0%	0.7%
4	-0.1%	-1.6%	0.0%	0.7%
12	-1.4%	-25.8%	-0.6%	11.7%
13	0.0%	0.5%	0.0%	-0.2%
14	-0.8%	1.4%	0.1%	-1.3%
23	0.8%	-0.9%	-0.1%	1.1%

Table S10. The energy differences between BS-DFT spin states and the high-spin state in cm^{-1} for complex **2** (a), the difference between $(\varepsilon_{BS,i} - \varepsilon_{HS})$ calculated with the help of derived J-parameters and actual BS-DFT values (b), and their relative errors (c)

a) $(\varepsilon_{BS,i} - \varepsilon_{HS})^{BS\text{-}DFT}$:

BS-state	PBE0	CAM-B3LYP	ωr^{2}SCAN	B3LYP
1	-55.735	-44.905	-64.153	-91.225
2	-53.453	-44.159	-64.690	-91.806
11‘	-119.504	-88.641	-130.771	-186.317
12	8.948	5.314	9.581	13.421

b) $(\varepsilon_{BS,i} - \varepsilon_{HS})^{J} - (\varepsilon_{BS,i} - \varepsilon_{HS})^{BS\text{-}DFT}$:

BS-state	PBE0	CAM-B3LYP	ωr^{2}SCAN	B3LYP
1	0.000	0.000	0.000	0.000
2	-5.039	-0.129	-0.557	-1.082
11‘	2.519	0.064	0.278	0.541
12	0.000	0.000	0.000	0.000

c) $[(\varepsilon_{BS,i} - \varepsilon_{HS})^{J} - (\varepsilon_{BS,i} - \varepsilon_{HS})^{BS\text{-}DFT}]/(\varepsilon_{BS,i} - \varepsilon_{HS})^{BS\text{-}DFT}$ (%):

BS-state	PBE0	CAM-B3LYP	ωr^{2}SCAN	B3LYP
1	0.0%	0.0%	0.0%	0.0%
2	9.4%	0.3%	0.9%	1.2%
11‘	-2.1%	-0.1%	-0.2%	-0.3%
12	0.0%	0.0%	0.0%	0.0%

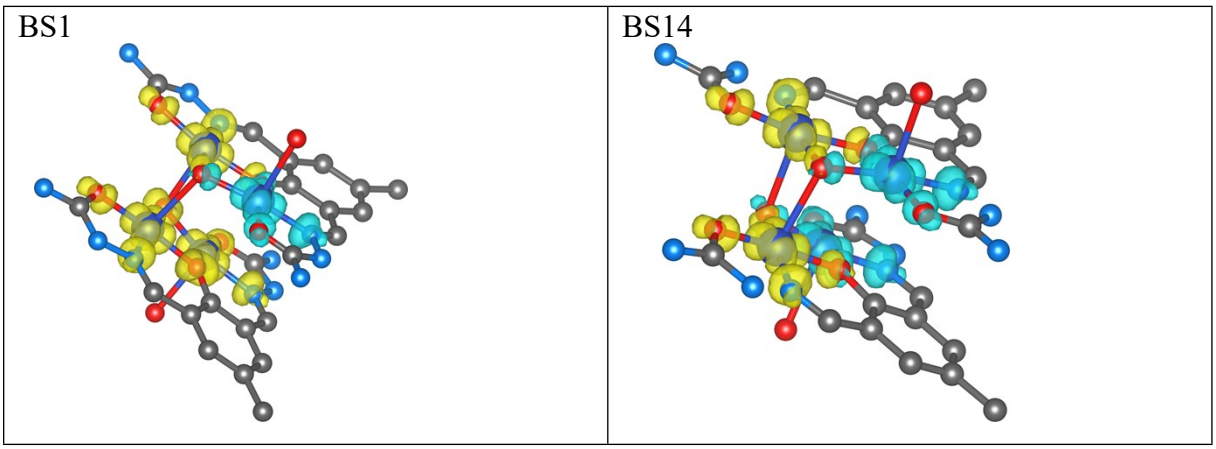

Figure S14. The calculated spin density distribution using CAM-B3LYP of complex **1** for selected BS-DFT states. Positive and negative spin density are represented by yellow and cyan surfaces, respectively. The isodensity surfaces are plotted with the cut-off value of 0.005 e_{a0}^{-3}. Hydrogen atoms are omitted for clarity.

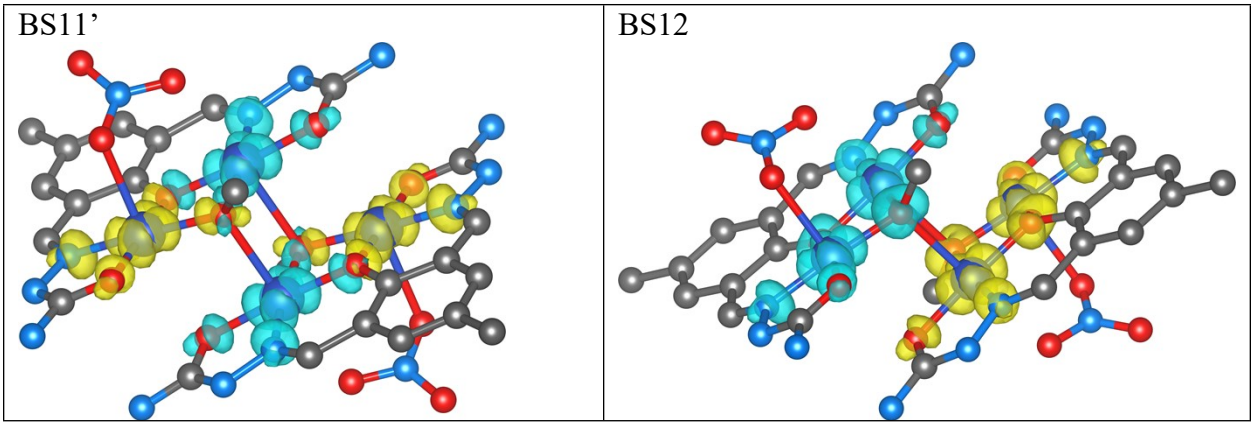

Figure S15. The calculated spin density distribution using CAM-B3LYP of complex **2** for selected BS-DFT states. Positive and negative spin density are represented by yellow and cyan surfaces, respectively. The isodensity surfaces are plotted with the cut-off value of 0.005 e_{a0}^{-3}. Hydrogen atoms are omitted for clarity.

Table S11. Comparison study of the obtained *Kcat* values with the recent literature-reported copper systems during catalytic oxidations

Complexes	K_{cat} (h^{-1})			**Reference**
	For Catechol oxidation	For 2-aminophenol oxidation	Solvent	
$[Cu_4L_2(\mu_3\text{-}OCH_3)_2](ClO_4)_2{\cdot}2H_2O$	13.32	23.04	DMSO	1
$[Cu_4L_2(H_2O)_2(\mu_3\text{-}OH)_2](NO_3)_2{\cdot}H_2O$	25.56	13.35	DMSO	
[Cu(L)(NCS) (ClO_4)]	25.20	78.28	MeOH	2
		21.17	MeCN	
$[Cu_3(L_5)(CH_3COO)_3]{\cdot}3H_2O$	7.5		MeOH	3
$[(CH_3CN)Cu(Ls)_2Cu]^{2+}$		11.1	MeOH	4
[CuLL′]$(NaClO4)_3$	58	50	MeOH	5
$[Cu_3L(OH)_3]$	25.67	65.5	DMF	6
$[Cu_4(L)_2(H_2O)_2(\mu_3\text{-}OH)_2](ClO_4)_4{\cdot}3H_2O$	12.08	0.101	MeOH-MeCN	Present work
$[Cu_4(L)_2(\mu\text{-}NO_3)_2(\mu_3\text{-}OMe)_2](NO_3)_2{\cdot}H_2O$	1.845	1.522		

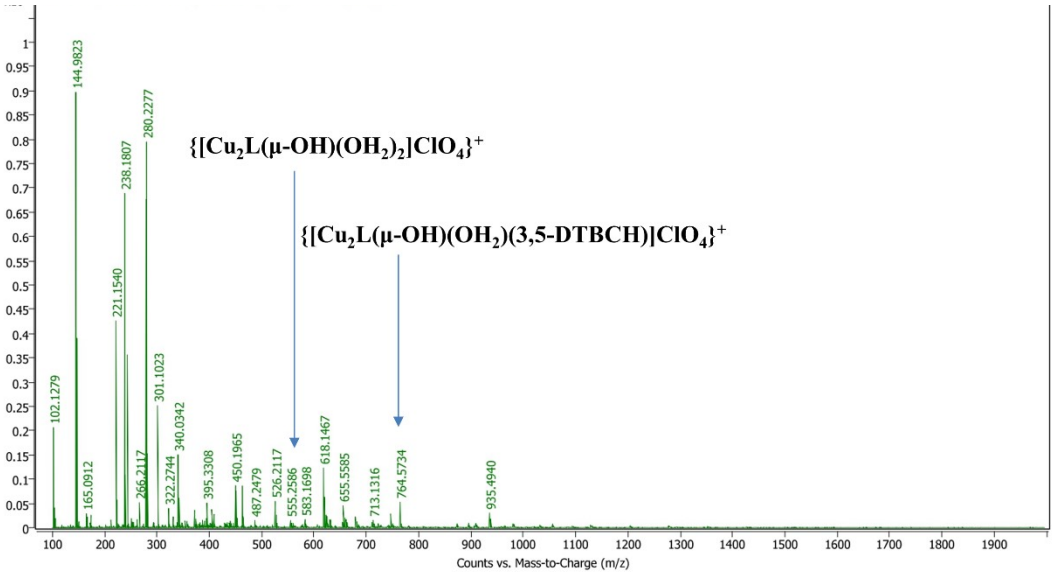

Figure S16. HRMS plot of **1** during oxidation of 3,5-DTBCH$_2$

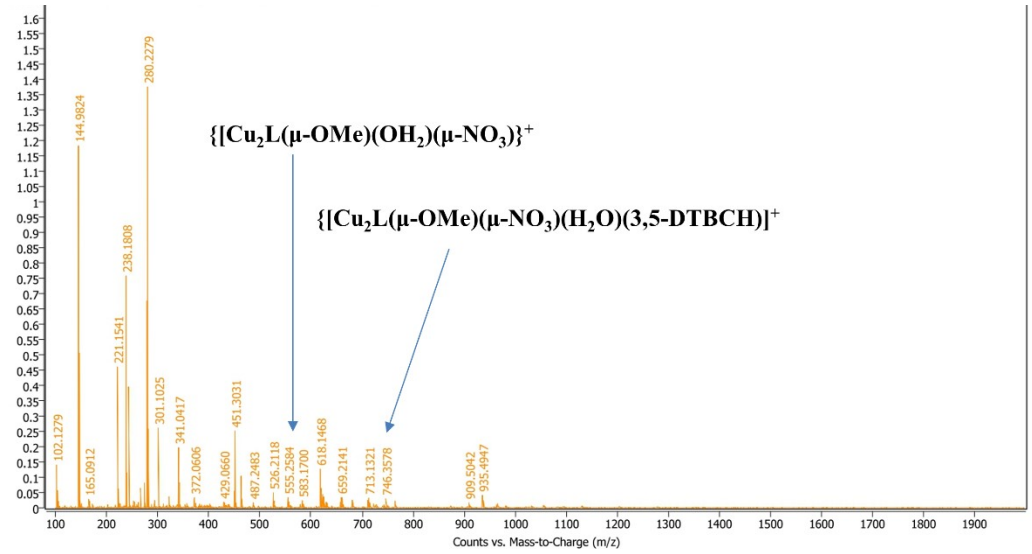

Figure S17. HRMS plot of **2** during oxidation of 3,5-DTBCH$_2$

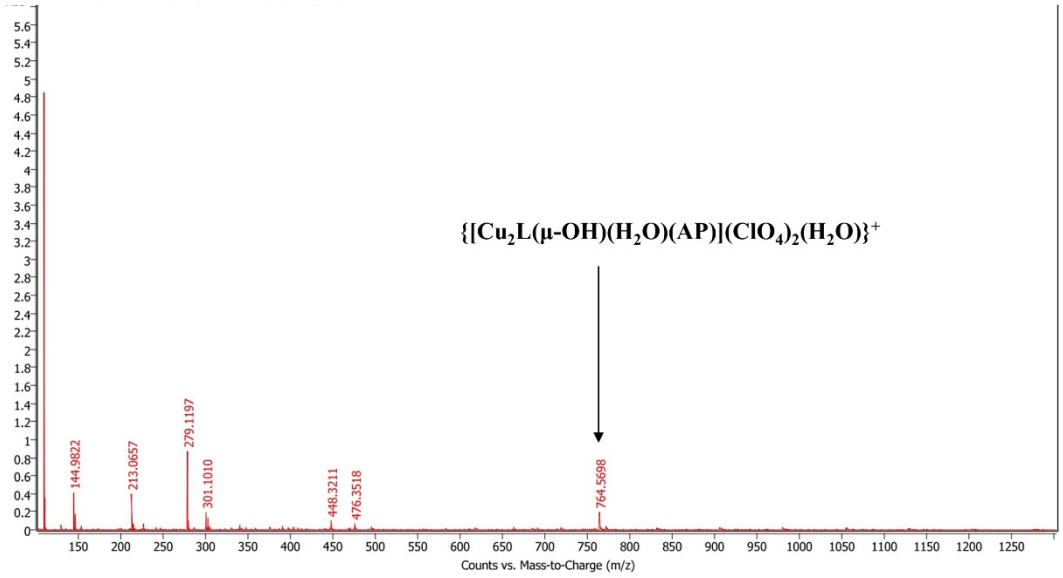

Figure S18. HRMS plot of **1** during oxidation of AP

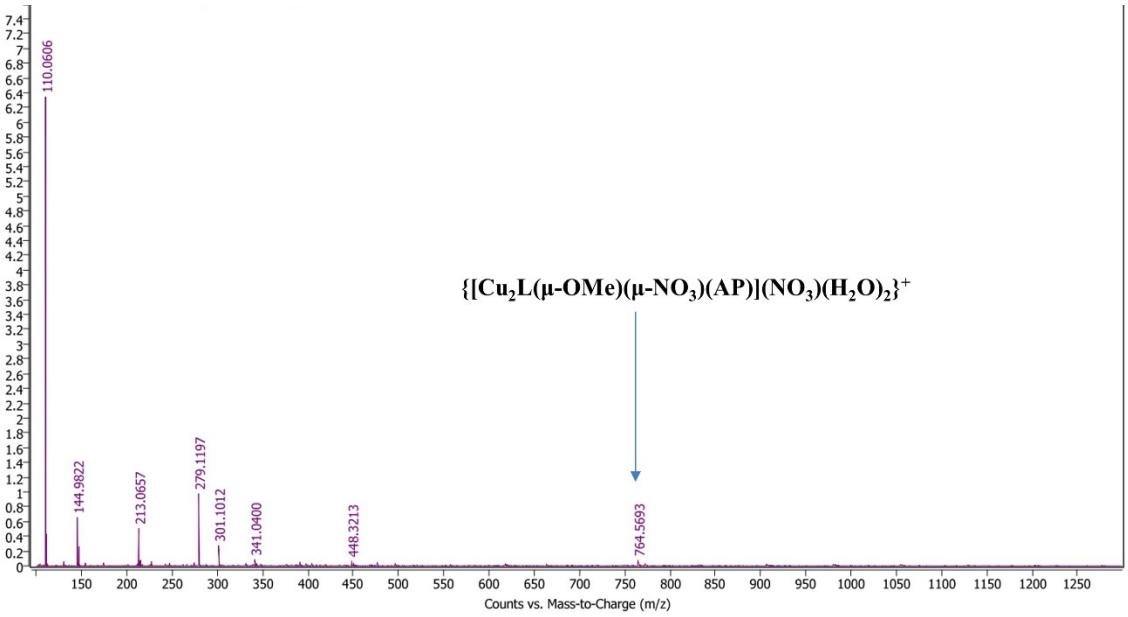

Figure S19. HRMS plot of **2** during oxidation of AP

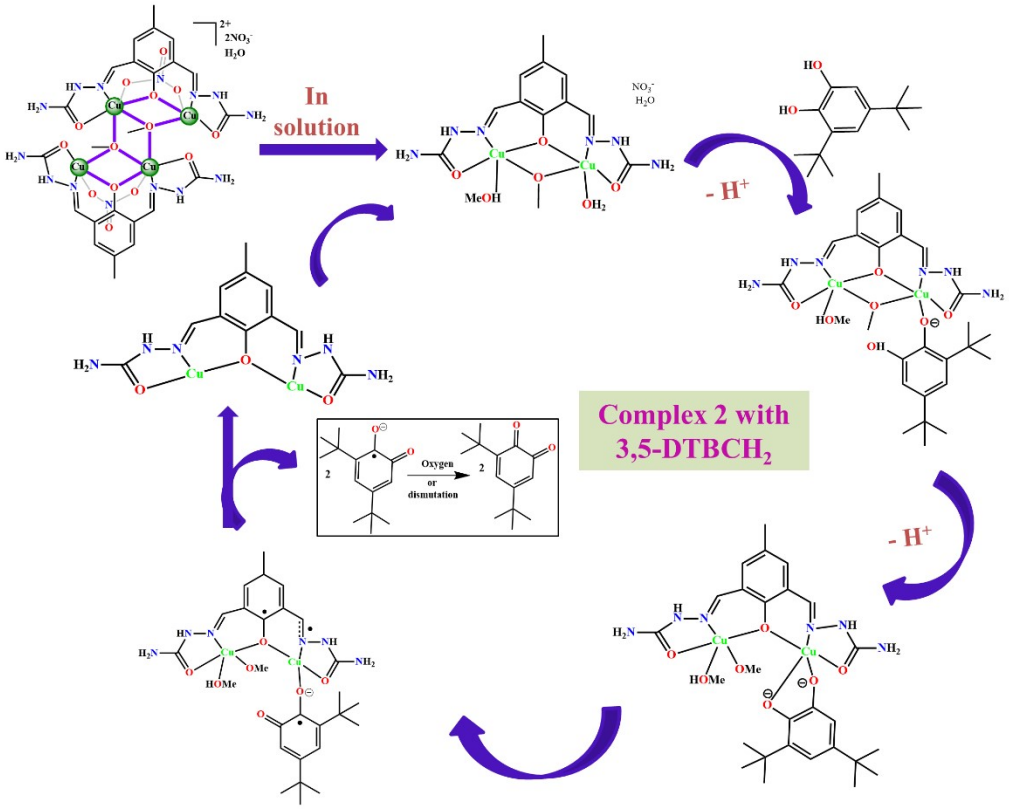

Figure S20. Proposed catalytic pathway of complex **2** for 3,5-DTBCH$_2$ oxidation

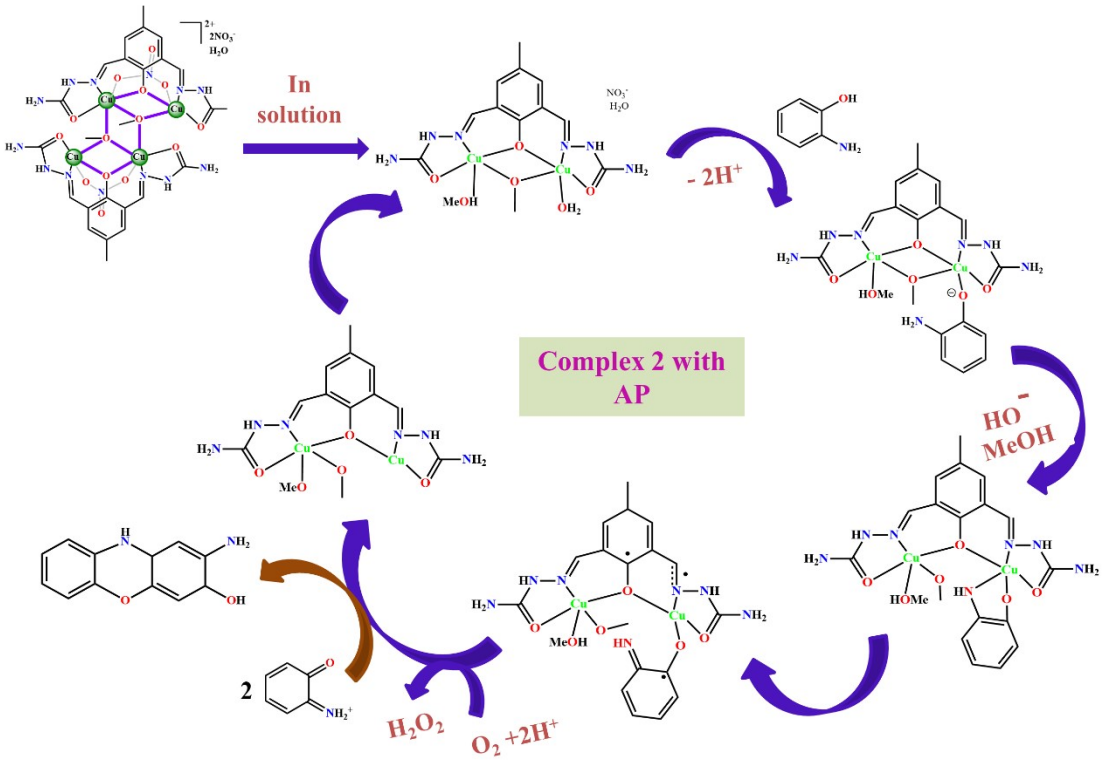

Figure S21. Proposed catalytic pathway of complex **2** for AP oxidation

References

1 A. Manna, Z. Jagličić and D. Ray, *Chem. Asian J.*, 2026, 0:e70497. https://doi.org/10.1002/asia.70497.

2 I. R. Chowdhury, A. Chatterjee, A. Mahanta, S. Jasimuddin and R. Ghosh, *Inorg. Chim. Acta,* 2024, **566**, 122006.

3 V.K. Bhardwaj, N. Aliaga-Alcalde, M. Corbella and G. Hundal, *Inorg. Chim. Acta,* 2009, **363**, 97-106.

4 T. Dutta, S. Mirdya, P. Giri and S. Chattopadhyay, *Polyhedron*, 2020, **175**, 114164.

5 A. E.M. M. Ramadan, S. Y. Shaban, M. M. Ibrahim, A. A. H. A. Rahman, S. A. Sallam, S. A. A. Harbie and W. Omar, *New J. Chem.,* 2020, **44**, 6331.

6 S. Nakul, M.G. Krishnendu, D. Senthurpandi, J. Mathew and N. V. Kulkarni, *Inorg. Chim. Acta,* 2025, **578**, 122550.